P2H.11

SIMULATIONS OF NEAR-GROUND HURRICANE WINDS INFLUENCED BY BUILT STRUCTURES

Christopher D. Karstens* and William A. Gallus, Jr.
Iowa State University, Ames, Iowa

1. INTRODUCTION

Hurricanes contain some of the most destructive winds on the planet. When a hurricane makes landfall, one of the most important forecasts to deliver accurately is that for winds. However, this remains a challenge due to many uncertainties in how the wind interacts with structures onshore. This study aims to provide forecasters with guidance in making such a forecast for four separate structural environments. By normalizing the velocity magnitudes to the predicted Weather Research and Forecasting (WRF) model 10 meter wind, results can be applied to hurricanes of varying intensity with relative ease. Also, by normalizing the velocity magnitudes to the WRF profile for a given elevation, the results offer utility in wind mitigation efforts.

2. METHODS

Our goal was to obtain a WRF simulation that did a reasonable job depicting the hurricane's actual intensity. Vertical wind profiles from this simulation could be used as input to the Fluent computational fluid dynamics software to simulate microscale flow of hurricane winds around built structures.

The dimensions of structures and corresponding wind tunnels also needed to be determined. The edge, face, and volume meshes could then be constructed at an appropriate size and exported for iterative solving in Fluent. The Fluent preprocessor Gambit was used for all domain and mesh creation.

2.1 *WRF*

Hurricanes Rita, Katrina, and Wilma were simulated using a 4-km grid spacing version of the WRF model. The domains were initialized using Global Forecast System (GFS) analyses approximately 24 hours prior to landfall. Each domain measured 400 x 350 points. Thirty-five vertical levels were used, with a higher concentration than standard near the surface to better resolve low-level winds.

Hourly model output was converted from netCDF format using ARWpost at 10 meter increments in the lowest 1-km. All model data were analyzed using the Grid Analysis and Display System (GrADS). The Tropical Cyclone Reports for each Hurricane were used for validation of the model's results (Knabb and Brown, 2007, Knabb et al., 2007, Pasch et al., 2007). The regions of highest forecasted 10 meter winds were identified, and vertical wind profiles from the first grid points on shore were extracted to initialize wind tunnels in Fluent.

The log wind equation was applied to the WRF profile for higher resolution initialization in Fluent. Additionally, these velocity values were used for normalization, which is discussed in section 2.4.

2.2 *Structural Domains & Meshing*

Suburban houses come in a complex array of designs and overall sizes. Rather than attempt to accurately depict a specific house design, simplified single story (Fig. 1a) and two story (Fig. 1b) house models were used to provide more applicability toward an average home. Additionally, suburban areas consist of many houses in a small, gridded area. The suburban array we considered consisted of a random assortment of the house models in Figures 1a and 1b (Fig. 1c). The dimensions of the structures are listed in Table 1.

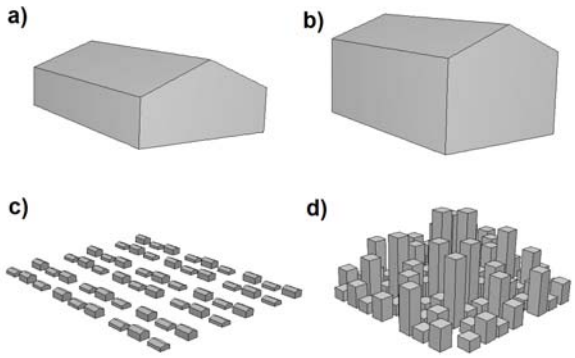

Figure 1. Visual display for the a) single story house, b) two story house, c) suburban array, and d) urban environment domains.

	1a	1b	1c	1d
Total Length	15	15	249	500
Total Width	10	10	180	500
Total Height	5	8	5-8	244
Roof Height	2	2	2	-

Table 1. Dimensions (m) of the structural domains listed in Figure 1.

To comprise the urban environment (Fig. 1d), the World Almanac and Book of Facts (2006) was used to reference building heights in the major coastal cities of

* *Corresponding author address:* Christopher D. Karstens, Iowa State Univ., Dept. of Geol. & Atmos. Sciences, Ames, IA; email: ckarsten@iastate.edu.

	1a	1b	1c	1d
Faces of Stucture(s)	0.25 Quad/Pave & Tri/Pave	0.25 Quad/Pave & Tri/Pave	1 Quad/Pave & Tri/Pave	1 – 5 Quad/Map & Boundary Layer
Bottom Face of Tunnel	2 – 0.25 Tri/Pave	2 – 0.5 Tri/Pave	2 – 1 Tri/Pave	10 – 5 Tri/Pave
Top Face of Tunnel	10 Quad/Map	10 Quad/Map	10 Quad/Map	20 Quad/Map
Side Faces of Tunnel	2 – 10 Tri/Pave	2 – 10 Tri/Pave	2 – 10 Tri/Pave	5 – 20 Quad/Map & Boundary Layer
Volume Mesh	Tet/Hybrid & Tgrid	Tet/Hybrid & Tgrid	Tet/Hybrid & Tgrid	Tet/Hybrid & Tgrid

Table 2. Resolution (m) and meshing schemes used for the structural domains listed in Figure 1.

the Southeast United States. These heights were used to construct a distribution, which was utilized as a guide in constructing the urban structures. Additionally, satellite photography of these cities was used to approximate the length and width of the urban domain. Additionally, a typical urban environment consists of large gaps, such as parking lots and open areas, randomly interspersed among the structures. To account for these areas, 20 percent of the urban environment was left as open spaces.

Each structural domain was positioned at five different orientations, including 0°, 22.5°, 45°, 67.5°, and 90°. This was done to simulate the effect of time, or a 90° changing of wind direction.

From the specifications shown in Table 1 and Figure 1, the dimensions of the wind tunnels could be determined. The wind tunnel needed to be sufficiently large to simulate the flow around the structure(s) without having a significant impact on the results.

Constructing edge, face, and volume meshes for these environments proved to be challenging. This was attributable to our desire to study the structure(s) effect on the winds in a large volume at a fine resolution. This resulted in high computational expense, which needed to be taken into careful consideration. The volume meshes required sufficient resolution to accurately resolve the flow characteristics around the structure(s). Thus, the spacing criteria listed in Table 2 were used for each domain.

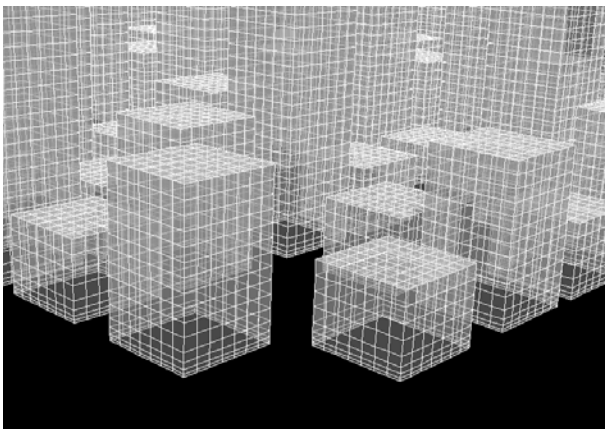

Figure 2. Boundary layer and face meshes on structure faces in the urban domain.

This set of criteria allowed the meshing scheme to create a fine resolution mesh around the structures, and gradually relax the resolution in areas away from the structures. The urban domain required slightly larger node spacing compared to the other domains, due to computational limitations. In order to maximize the resolution around the structures and near the ground, boundary layers were placed at the bottom of each structure's face (Fig. 2).

2.4 *Solving & Post Processing*

Fluent 6.3 was used to iteratively solve the flow simulations. All of the domains were run in Reynolds-averaged Navier-Stokes (RANS) mode using the k-ε turbulence model, based on results from Hanna et al. (2006). Thus, the results provide time averaged 3-D variability in close proximity to the structures.

The WRF profile was used to initialize the velocity inlet, with a 1-meter resolution near the ground. Additionally, a roughness parameter was placed on the bottom floor of the tunnel in order to maintain the original properties of the WRF profile. The single story house, two story house, and suburban simulations were able to converge, while the urban simulation was run until the residuals appeared quasi-steady.

High resolution horizontal plane grids with even spatial distribution were created at vertical increments of 1 meter. The area over which the planes were created varied for each domain. Planes measuring 24 x 30 meters were created for the single story and two story house domains. This equates to a lot area of approximately 7,750 ft^2, which might be typical in a suburban area. The suburban and urban domains used planes that encompassed the interior of the structural environment. The intention was to gain a sense of how the incoming wind is affected by the complex structural arrays.

Two separate types of normalizing were conducted to achieve two purposes. First, each plane was normalized to the ambient incoming wind for each elevation specified (WRF profile). This gives an indication of how the structure is influencing the flow

relative to the incoming WRF profile. Second, all horizontal grids were normalized to the WRF's predicted 10-meter wind. This gives an indication of how the structure is influencing the flow relative to WRF's 10-meter forecasted wind speeds. Since model forecast charts for hurricanes typically include the predicted 10 meter winds, this type of normalizing might be more beneficial to the forecaster.

3. RESULTS

The results have been broken into three sections, including WRF, normalizing to the WRF profile, and normalizing to the WRF 10 meter forecasted wind. For both normalizing sections, only the 0 degree orientation is addressed due to compelling similarities between the five orientations for each domain.

3.1 *WRF*

As evident in figure 3, the 4-km version of the WRF underpredicted the landfalling intensity of each hurricane. In our best simulations, the central minimum pressure was 10 to 15 mb weaker at landfall than the observed value. These results were somewhat expected, which is likely due to the coarseness of the resolution of the model data used to initialize WRF. As Kimball and Dougherty (2006) point out, there are three essential elements to successful hurricane modeling, which include grid resolution, physical parameterizations, and model initialization.

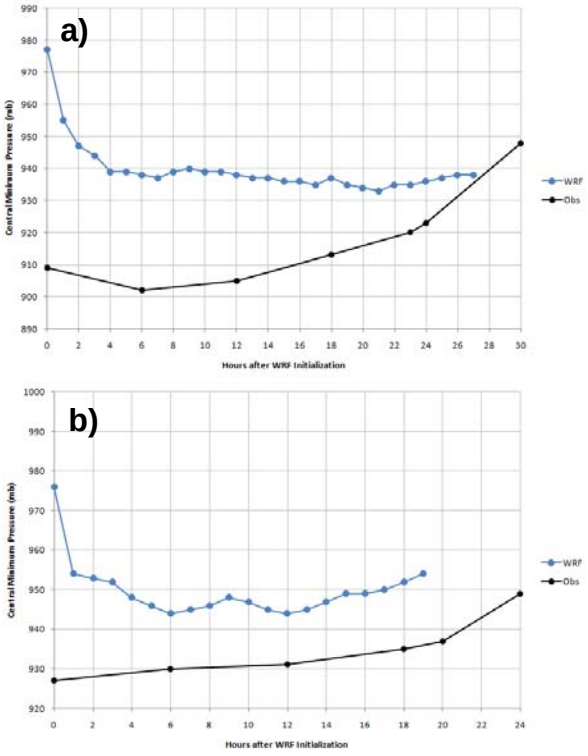

Figure 3. Time series of central minimum pressure near landfall for a) Hurricane Katrina and b) Hurricane Rita.

Our initial hope was to improve the model initialization by utilizing WRF 3-Dimentional Data Assimilation (3DVAR). Barker et al. (2004) show that assimilating observations into model initialization can greatly improve a hurricane forecast. However, due to computational issues the current version of WRF-3DVAR is incompatible with our computer systems. Thus, we were unable to perform any data assimilation to improve our model initialization. The next release of the 3DVAR code is expected to be compatible with our system. We will attempt to implement this release, which will hopefully lead to improved model initialization. In an attempt to improve our present simulations, we enhanced the grid resolution by including a 2-km nested grid. However, results from this simulation were nearly identical to the 4-km simulations. Of the three hurricanes simulated thus far, results from our Hurricane Katrina simulations showed the best comparison to observations.

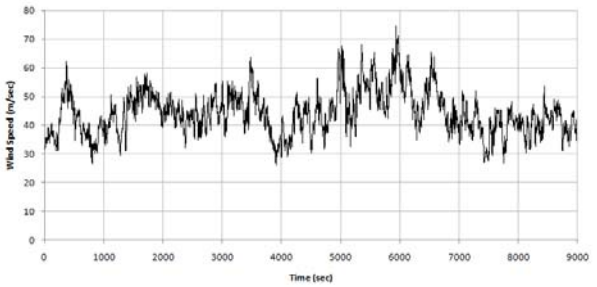

Figure 4. Time series of the observed 10-meter wind from an instrument tower deployed in Hurricane Katrina at Belle Chase, LA.

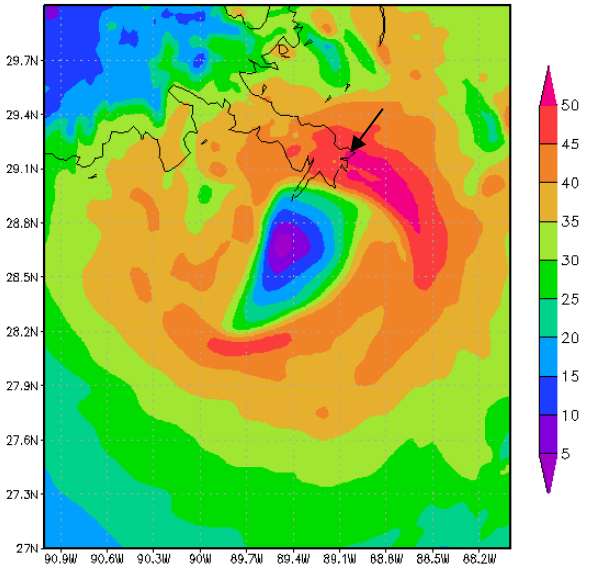

Figure 5. WRF 10 meter winds forecast for Hurricane Katrina. Arrow denotes location of wind profile extracted for Fluent simulations.

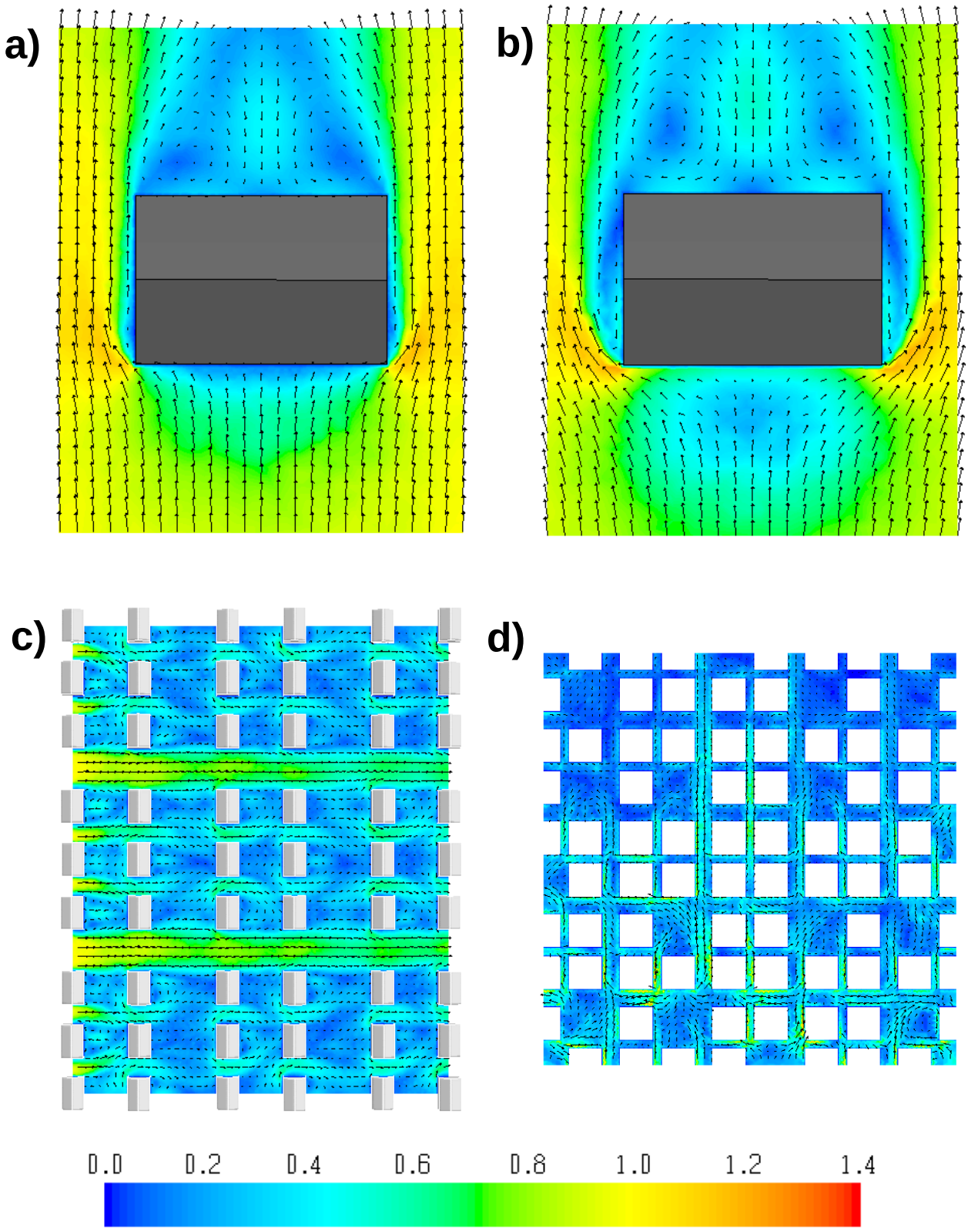

Figure 6. Horizontal grids of normalized 2-meter winds for the a) single story house, b) two story house, c) suburban, and d) urban domains.

WRF's underprediction of the central minimum pressure in each hurricane simulation results in a subsequent underprediction of the wind speeds. The observed winds from Hurricane Katrina (Fig. 4) show persistent speeds in the 30 to 60 ms^{-1} range, with several peaks in the 60 to 70 ms^{-1} range. However, results from our WRF simulation show maximum onshore winds approaching 50 ms^{-1} (Fig. 5). While this is notably weaker than the observed peaks of Fig. 4, it does lie within the persistent range. Thus, we determined that a profile in the region of maximum predicted onshore winds would be sufficient for our Fluent simulations.

3.2 *Normalized to the WRF profile*

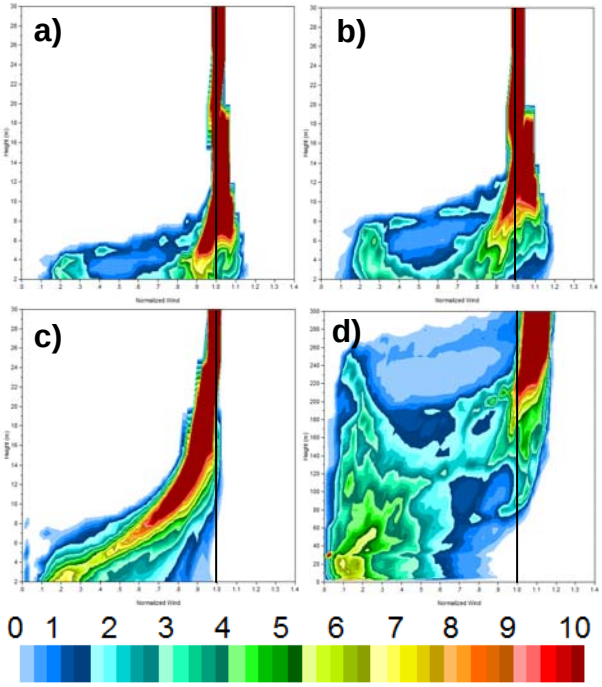

Figure 7. Distribution contour plots (0-10%) normalized to the initializing WRF profile for the a) single story house, b) two story house, c) suburban, and d) urban domains.

Fig. 6 depicts airflow around the structural environments with the normalized values contoured. These plots are used to aid in interpreting Fig. 7, which shows normalized distribution contour plots from high resolution planes generated for each domain, oriented at 0 degrees.

For the single story house, there are 3 general peaks evident near the ground (Fig. 7a). The first is a reduction to between 20 to 30 percent of the ambient value. This peak corresponds to the wake region behind the structures (blue areas of Fig. 6a). It can be noted that the height of this region corresponds well to the height of the structure. The second is a reduction to between 80 to 100 percent of the ambient value, which corresponds to regions near the outer edges of the planes that are subtly influenced by the structures (yellow and green areas of Fig. 6a). The last peak, which is an increase to 110 to 120 percent of the ambient value, is more evident in the lowest two to twenty meters. This peak appears to correspond to the corners of the structure on the side closest to the incoming winds, (orange areas of Fig. 6a) and to regions just above the structure, where winds are accelerating around the structure.

The distribution plot for the two story house (Fig. 7b) shows much similarity to the plot for the single story house, (Fig. 7a) with a few exceptions. First, the depth to which the profile is influenced is now slightly deeper, which once again corresponds to the height of the structure. Secondly, the upper peak of winds accelerated to 110 to 120 percent is less apparent near the ground. This is illustrated in Fig. 6b, which shows smaller spatial coverage of these values compared to Fig. 6a.

Results from the suburban domain (Fig. 7c) are much different than either of the single house domains. This is primarily the result of considering the impact of several structures on the WRF profile versus just a single structure. From Fig. 7c, virtually the entire profile is decelerated in the lowest 20 meters. At the two meter elevation, a large spectrum of wind values is present, with a substantial peak at 20 to 30 percent. This is illustrated in Fig. 6c, which shows large variations in the normalized values, with a majority corresponding to the 20 to 30 percent range (blue contours).

The urban structural environment undoubtedly had the greatest impact on the WRF profile. Fig. 7d shows a significant range in the wind speeds within the structural region, with a broad peak occurring in the 10 to 30 percent range at the two meter elevation. This is evident in Fig. 6d by the significant spatial coverage of values in this range. Additionally, this peak is evident up to an elevation of about 150 meters, and gradually diminishes as the elevation reaches 300 meters. Additionally, a secondary peak develops in the 100 to 120 percent range at an elevation of 70 to 80 meters and persists up to an elevation of 300 meters.

3.3 *Normalized to the WRF 10 meter wind*

Lastly, the distributions were normalized to the WRF 10 meter wind for potential utility in forecasting hurricane winds (Fig. 8). In general, these plots reflect the same general characteristics as the plots in Fig. 7, only skewed logarithmically with height. The result is a general reduction in the winds below 10 meters and an increase above 10 meters.

While the main characteristics of Fig. 7 are evident in Fig. 8, the implications of these results are much different. Specifically, these charts show how well the WRF 10 meter wind compares to Fluent's depiction of flow around the four structural domains. This is visualized in Fig. 8, where the vertical black line represents the 10-meter forecast, and the contoured distributions represent Fluent's depiction of the flow.

Forecasting specifically for the 10 meter elevation, this approach might be reasonable for the single story

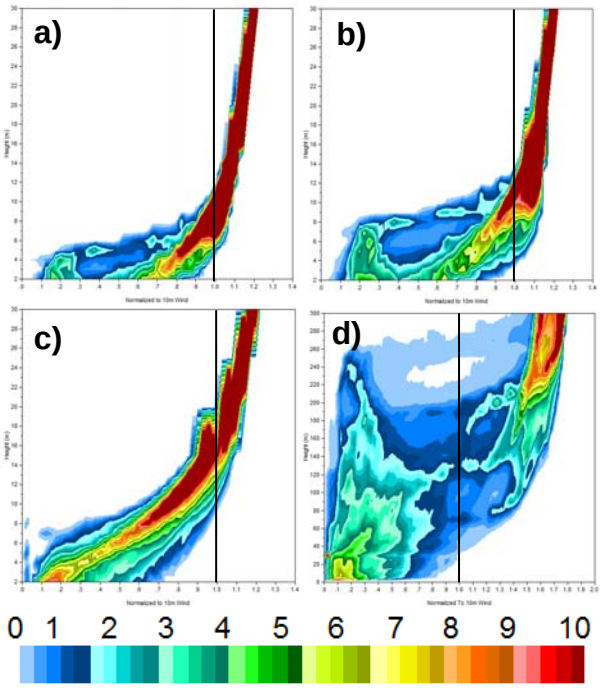

Figure 8. Distribution contour plots (0-10%) normalized to the WRF forecasted 10 meter wind for the a) single story house, b) two story house, c) suburban, and d) urban domains.

and two story house domains (Figs. 8a and 8b). These figures indicate that best correspondence occurs in the 6 to 11 meter layer for both domains, with an overprediction below 6 meters ranging between 10 to 80 percent of WRF's 10 meter value. An underprediction is evident above 11 meters, with the winds projected to be 10 to 20 percent higher.

However, 10 meter wind forecasts do not compare well to the suburban and urban flow depiction from Fluent (Figs. 8c and 8d). For the suburban domain (Fig. 8c), the 11 to 18 meter elevation Fluent winds correspond well to the WRF 10 meter wind. At the 10 meter elevation, the winds are 70 to 90 percent of the predicted 10 m value. Additionally, an overprediction is evident below 11 meters, ranging from 10 to 50 percent of WRF's 10 meter value. An underprediction is evident above 18 meters, with the winds projected once again to be 10 to 20 percent higher.

Comparison in the urban domain is poor. Fig. 8d shows that virtually all of the projected winds below 300 meters are either significantly under of over WRF's predicted 10 meter value. At the 10 meter elevation, an overprediction is evident. Below 100 meters, the winds range from 10 to 70 percent of WRF's 10 meter value. Above 100 meters, a significant acceleration is observed, more so than any other domain. Winds here range between 40 to 80 percent higher than WRF's forecasted 10 meter wind.

Since the WRF 10 meter predicted wind may not be applicable throughout the depth of these built environments, scaled adjustments should be made to accommodate for the profile's interaction with the structures. Based on these results, a forecaster analyzing a 10-meter wind chart could make a 60 to 80 percent adjustment to forecast the 2-meter winds in close proximity to a single story or two story structure, and a 10 to 40 percent adjustment in proximity to a suburban and urban environment.

4. CONCLUSIONS

While our simulations underpredicted the landfalling intensity of each hurricane, the WRF forecasted 10-meter winds from our Hurricane Katrina simulations compare well with winds measured by instruments placed in Katrina's path. While these results appeared reasonable for subsequent Fluent simulations, our goal remains to improve our hurricane simulations. This ideally will be achieved by utilizing WRF-3DVAR.

Results from our Fluent simulations show that built environments of various characteristics have a unique impact on the ambient, incoming flow. In general, the structural environments act to decrease the magnitude of the incoming profile in regions at or below the elevation of the structure(s), and act to slightly increase winds at higher elevations. An exception is evident in the urban domain, where a substantial acceleration is apparent above 75 to 80 meters.

While the general characteristics of Fig. 7 are evident in Fig. 8, the implications of these results are much different. If a forecaster were to use the model's predicted 10 meter value to forecast the 10-meter wind near a single story or two story house in open terrain, the forecast could potentially verify pretty well. Doing so for a suburban or urban setting may not. Additionally Fig. 8 shows at which elevations the WRF 10 meter wind forecast could potentially verify. Using WRF's predicted 10 meter value to forecast wind at 2 meters would also result in error for the four structural environments considered in this study. Adjustments are recommended when forecasting for each built environment.

Given that our Fluent simulations were solved to a steady state, the results shown in Figs. 7 and 8 give time averaged 3-D variability. For complex built environments, it is hypothesized this type of simulation might smooth out brief, small-scale accelerations that occur around the individual structures. Thus, for future work, unsteady simulations are being considered.

5. REFERENCES

Barker, D. M., W. Huang, Y. R. Guo, and Q. N. Xiao, 2004: A three-dimensional data assimilation system for use with MM5: Implementation and initial results. *Mon. Wea. Rev.,* **132,** 897–914.

Hanna S.R., M.J. Brown, F.E. Camelli, S. Chan, W.J. Coirier, O.R. Hansen, A.H. Huber, S. Kim, and R.M. Reynolds, 2006: Detailed simulations of atmospheric flow and dispersion in urban downtown areas by computational fluid dynamics (CFD) models—an

application of five CFD models to Manhattan. *Bull. Amer. Meteor. Soc.,* **87,** 1713–1726.

Kimball, S.K., and F.C. Dougherty, 2006: The sensitivity of idealized hurricane structure and development to the distribution of vertical levels in MM5. *Mon. Wea. Rev.,* **134,** 1987–2008.

Knabb, R.D., and D.P. Brown, cited 2007: Tropical cyclone report Hurricane Katrina 23-30 August 2005. [Available online at http://www.nhc.noaa.gov/pdf/TCR-AL122005_Katrina.pdf.]

_____, D.P. Brown and J.R. Rhome, cited 2007: Tropical cyclone report Hurricane Rita 18-26 September 2005. [Available online at http://www.nhc.noaa.gov/pdf/TCR-AL182005_Rita.pdf.]

Pasch, R.J., and E.S. Blake, H.D. Cobb III, and D.P. Roberts, cited 2007: Tropical cyclone report Hurricane Wilma 15-25 October 2005. [Available online at http://www.nhc.noaa.gov/pdf/TCR-AL252005_Wilma.pdf .]

World Almanac Education Group, 2006: *World Almanac and Book of Facts.* World Almanac Education Group, 1008.